http://www.pjbs.org

PJBS

ISSN 1028-8880

Pakistan Journal of Biological Sciences

ANSInet
Asian Network for Scientific Information
308 Lasani Town, Sargodha Road, Faisalabad - Pakistan

OPEN ACCESS Pakistan Journal of Biological Sciences

ISSN 1028-8880
DOI: 10.3923/pjbs.2025.749.764

Research Article
Antibacterial and Anticancer Properties of Anthraquinone Derivatives from *Streptomyces kunmingensis* BH111, an Isolate from Beehive

[1]Thongchai Taechowisan, [1]Thanaporn Chuen-Im and [2]Waya S. Phutdhawong

[1]Department of Microbiology, Faculty of Science, Silpakorn University, Nakhon Pathom 73000, Thailand
[2]Department of Chemistry, Faculty of Science, Silpakorn University, Nakhon Pathom 73000, Thailand

Abstract

Background and Objective: The persistent global threats of antimicrobial resistance and cancer necessitate the discovery of novel chemical entities, a search where actinomycetes from unique environments are critical. To discover new therapeutics, this study investigated actinomycetes from the *Apis florea* beehive environment, aiming to identify a promising strain and structurally characterize its antibacterial and anticancer metabolites. **Materials and Methods:** Actinomycetes were isolated from five *Apis florea* beehives. Strain identification was performed using morphological, chemotaxonomic and dual-gene sequencing (16S rRNA and *gyr*B). Metabolites were purified and biological activity was assessed using MIC/MBC (antibacterial) and MTT cytotoxicity assays. The mechanism was explored via molecular docking against Topoisomerase II, complemented by ADMET prediction. **Results:** The most active isolate, BH111, was identified as *Streptomyces kunmingensis*. It produced two anthraquinone derivatives: Resistomycin (Compound **1**) and tetracenomycin D (Compound **2**). These compounds demonstrated selective, potent antibacterial activity against Gram-positive strains (MIC and MBC values ranged from 16 to 32 and 128 to 256 µg/mL, respectively) and significant cytotoxicity against tested cancer lines (IC_{50} values ranged from 10.72 to 27.57 µg/mL). Docking results supported Topoisomerase II inhibition. However, low selectivity indices and ADMET flags (CYP450, hepatotoxicity) were noted. **Conclusion:** *Streptomyces kunmingensis* BH111 is the first strain of this species reported to produce resistomycin and tetracenomycin D from a beehive source. While these anthraquinone derivatives are promising drug scaffolds due to their potent antibacterial and topoisomerase-inhibiting anticancer activities, significant therapeutic optimization is required to enhance selectivity and mitigate predicted toxicological risks.

Key words: Anthraquinone derivatives, antibacterial activity, anticancer activity, beehive, *Streptomyces kunmingensis* BH111

Citation: Taechowisan, T., T. Chuen-Im and W.S. Phutdhawong, 2025. Antibacterial and anticancer properties of anthraquinone derivatives from *Streptomyces kunmingensis* BH111, an isolate from beehive. Pak. J. Biol. Sci., 28: 749-764.

Corresponding Author: Thongchai Taechowisan, Department of Microbiology, Faculty of Science, Silpakorn University, 6 Rajamankanai Road, Nakhon Pathom 73000, Thailand

Competing Interest: The authors have declared that no competing interest exists.

Data Availability: All relevant data are within the paper and its supporting information files.

INTRODUCTION

Actinomycetales represent a widespread and ecologically vital order of bacteria, inhabiting a vast array of environments globally. These organisms are key components of soil ecosystems, where their capacity to decompose complex organic matter is essential for nutrient cycling. Their ecological roles extend to symbiotic relationships, notably as nitrogen fixers in partnerships with plants. Furthermore, actinomycetes are highly adaptable, thriving in diverse aquatic settings, including marine sediments, salt marshes, lakes and river systems. They are also recognized as endosymbionts within animal guts, where they can aid in host digestion, highlighting their profound ecological significance and versatility[1].

A specific focus has recently been placed on actinomycetes associated with beehives (e.g., worker bee tissue, brood cells and hive materials)[2,3]. The presence of these bacteria in the apiary environment is noteworthy due to their well-established ability to produce bioactive molecules. Actinomycetales are prolific sources of natural products, including a variety of antimicrobial compounds such as antibiotics, enzymes and antifungals. These compounds are thought to be crucial for microbial competition and survival in natural habitats and could potentially offer the host bees protection against bacterial pathogens[2,4]. Recent research has confirmed this potential, with the isolation of a *Streptomyces* strain (*AmelAP-1*) from beehive pollen stores. This strain was found to inhibit the growth of the serious entomopathogen *Paenibacillus larvae*, with the active molecule identified as piceamycin[2].

The current study builds on this foundation by investigating actinomycetes isolated from the beehives of *Apis florea*. Their antibacterial activity was first assessed. While the BH111 strain showed promising activity, its taxonomic classification currently lacks comprehensive data beyond basic morphological, physiological and chemotaxonomic profiles. Moreover, while successfully isolating and elucidating the chemical structure of a major antibacterial compound, several critical knowledge gaps remain. A thorough investigation is still needed to precisely define the compound's mechanism of antibacterial action and its full spectrum of activity against a broader panel of clinically relevant, multidrug-resistant (MDR) strains. Finally, preliminary assessments of cytotoxicity were conducted on Vero, MDA-MB-231, HeLa and HepG2 cell lines; however, a more robust toxicological profile, including non-cancerous human cell lines and *in vivo* models, is essential to establish the compound's potential therapeutic value and safety.

MATERIALS AND METHODS

Study area: This research was conducted within the Department of Microbiology and Chemistry at Silpakorn University, Nakhon Pathom, Thailand. Experimental procedures were carried out over a period spanning June, 2024 to July, 2025.

Sample collection and actinomycete isolation: Five *Apis florea* beehives were collected by local beekeepers from the Circle House in Kanchanaburi, Thailand (14.02762 N, 99.51710 E). Samples were immediately placed in sealed plastic bags to prevent contamination and promptly transported to the Silpakorn University Laboratory. For processing, a 10 g aliquot from each hive sample was randomly selected, combined with 90 mL of phosphate-buffered saline (PBS) in a stomacher bag and mechanically homogenized for 10 min. The resulting suspension was plated by spreading 100 µL onto humic-acid vitamin agar supplemented with the fungal and bacterial inhibitors cycloheximide (50 g/mL) and nalidixic acid (20 g/mL), respectively. Plates were incubated at 32°C for two weeks. Presumptive actinomycete colonies were selected based on characteristic visual morphology, subcultured onto International *Streptomyces* Project medium 2 (ISP-2) and purified for further analysis.

Screening of antibacterial actinomycetes and bioactive compound extraction: A total of 39 actinomycete isolates were screened for antimicrobial activity against a panel of eight bacterial strains: The Gram-positive species *Bacillus cereus* TISTR687, *B. subtilis* TISTR008, *Staphylococcus aureus* TISTR885, *S. epidermidis* TISTR518 and a clinical isolate of Methicillin-resistant *Staphylococcus aureus* (MRSA) strain Sp3, as well as the Gram-negative species *Escherichia coli* TISTR887, *Pseudomonas aeruginosa* TISTR1287 and *Salmonella typhimurium* TISTR2519. The soft-agar overlay method[5] was utilized to test antimicrobial activity. The resulting inhibition zones were measured following incubation. All screening experiments were performed in triplicate. Strain BH111 was selected for further study as it exhibited the most potent antibacterial properties. Initial classification of BH111 was performed via standard morphological, physiological and chemotaxonomic characterizations[6]. To obtain sufficient material, strain BH111 was cultured on 500 ISP-2 Petri dishes and incubated for 21 days at 32°C. Metabolites were extracted from the culture medium following an established procedure[7]. Briefly, the agar

medium was fragmented and subjected to exhaustive extraction with ethyl acetate (3×5 L). The collected organic solvent was pooled and concentrated to dryness using a rotary evaporator, yielding 9.50 g of a dark brown solid crude extract. The crude extract was subsequently divided into two portions. Part 1 was re-suspended in 5 mL of sterile Dimethyl Sulfoxide (DMSO) to a final concentration of 10.24 mg/mL and stored at -20°C for use in antibacterial and cytotoxicity assays. Part 2 was re-suspended in Dichloromethane (CH_2Cl_2) for subsequent compound purification and structural analysis. A preliminary assay was performed using Thin-Layer Chromatography-Direct Bioautography (TLC-DB)[8].

Identification of the selected strain: Strain BH111 was characterized by observing morphological characteristics after 21 days on ISP-2 medium, including the presence and color of aerial mycelium, spore mass color, distinctive reverse colony color, diffusible pigment production and the morphology of the sporophores and spore chains. Chemotaxonomic analysis, which determined the isomers of diaminopimelic acid and whole-cell sugars and the investigation of physiological characteristics were performed according to standard protocols[9,10].

16S rRNA, *gyr*B gene sequencing and phylogenetic analysis of the selected strain: The selected isolate was grown in 50 mL of ISP-2 broth at 32°C in a shaker (150 rpm) for 7 days. Cells were harvested by centrifugation (6,000 rpm for 20 min) and washed three times with PBS. Genomic DNA was extracted and the 16S rRNA and *gyr*B genes were amplified using established methods[11,12]. The primers used were: 16S rRNA: A7-26f (5'-CCGTCGACGAGCTCAGAGTTTGATCCTGGCT CAG-3') and B1523-1504r (5'-CCCGGGTACCAAGCTTAAGGAGG TGATCCAGCCGCA-3'), *gyr*B: UP1f (5'-GAAGTCATCATGACCGTT CTGCAYGCNGGNGGNAARTTYGA-3') and UP2r (5'-AGCAGGG TACGGATGTGCGAGCCRTCNACRTCNGCRTCNGTCAT-3').

The PCR products were purified using a QIAquick gel extraction kit (Qiagen, Germany) and sequenced via the Sanger method at 1st BASE, Singapore. Sequence similarity was confirmed using the NCBI BLAST tool (https://blast.ncbi.nlm.nih.gov/Blast.cgi). Sequences of closely related type strains were retrieved from GenBank, aligned using Clustal W and a phylogenetic tree was constructed using the Neighbor-Joining method in MEGA 11 software[13]. *Microbispora corallina* DF-32 and *Microbispora corallina* JCM 10266 served as outgroups for the 16S rRNA and *gyr*B trees, respectively.

Compound purification and characterization: For purification, 9.21 g of the crude extract was subjected to silica gel column chromatography (Merck, 0.040-0.063 mm). The elution gradient progressed from Dichloromethane (CH_2Cl_2) to Methanol (MeOH). The desired fractions were specifically eluted with 4-5% MeOH in CH_2Cl_2. Final purification was achieved using thin-layer chromatography (TLC) with a CH_2Cl_2:EtOAc (1:5) solvent system, which successfully yielded 10.64 mg of Compound **1** and 14.37 mg of Compound **2**. The structures of the isolated compounds were determined using a suite of spectroscopic techniques. Melting points were measured using a Stuart SMP20 apparatus (Cole-Parmer). The UV spectra were recorded on a PerkinElmer Lambda 35 spectrophotometer (PerkinElmer) (600 MHz) and (125 MHz) spectra were acquired using a Bruker Avance III NMR spectrometer (Bruker). Finally, molecular weight was determined via a POLARIS Q mass spectrometer (Thermo Fisher Scientific).

Determination of minimum inhibitory concentration (MIC) and minimum bactericidal concentration (MBC): The minimum inhibitory concentration (MIC) and minimum bactericidal concentration (MBC) for both the crude extract and the purified compounds were determined against the relevant bacterial strains using the standard broth microdilution method[14]. Chloramphenicol (Thermo Fisher Scientific, Massachusetts, USA) was used as the positive control.

Determination of cytotoxicity activity: The cytotoxicity of the crude extract and the purified compounds was assessed via the MTT assay[15]. Both samples were tested against three cancer cell lines: human breast carcinoma (MDA-MB-231), human cervical carcinoma (HeLa) and human hepatocellular carcinoma (HepG2). A concentration range from 1 to 512 g/mL was used for all assays. The African green monkey kidney (Vero) cells were included as a non-cancerous control cell line to determine selectivity.

The selectivity index (SI) was calculated as the ratio of the (50% cell growth inhibition concentration) in the Vero cell line to that in each respective cancer cell line, where a higher SI value indicates greater selectivity toward cancer cells. Doxorubicin hydrochloride (Thermo Fisher Scientific, Massachusetts, USA) served as the positive control for the cytotoxicity assay.

Molecular docking and ADMET studies: Given that the purified compounds were identified as anthraquinone derivatives-a class of molecules known to act as potential inhibitors of topoisomerase II, a critical cancer drug target[16], studies were warranted.

The 3D structures of the ligands (Compound **1:** Resistomycin and Compound **2:** Tetracenomycin D) were modeled and energy-minimized using UCSF Chimera software[17]. The target protein, human topoisomerase II (PDB ID: 4G0U), was retrieved from the Protein Data Bank (PDB). Molecular docking simulations were performed using AutoDock Vina within UCSF Chimera. A 25×25×25 A° cubic grid box was centered at the protein's active site, defined by the co-crystallized inhibitor (amsacrine, ASW). Results were reported as binding affinities (kcal/mol), with the lowest-energy conformation selected as the optimal pose. Interactions (e.g., hydrogen bonds, hydrophobic interactions) were visualized and analyzed using Discovery Studio Visualizer (BIOVIA, San Diego, California, USA). Doxorubicin was used as a positive control.

Finally, prediction of ADMET (Absorption, Distribution, Metabolism, Excretion and Toxicity) properties was carried out using the online platforms SwissADME[18], Pre-ADMET[19] and pkCSM[20]. The ADMET properties of known inhibitors were used for comparative analysis.

Statistical analysis: All biological experiments were performed in three replicates. Data are expressed as the Mean Standard Deviation (SD). Statistical analysis was conducted using SPSS for Windows, version 11.01 (SPSS Inc., Chicago, Illinois, USA). One-way Analysis of Variance (ANOVA) followed by Tukey's test was used to determine statistically significant differences between groups. Differences were considered significant at a p-value <0.05.

RESULTS

A total of 39 actinomycete isolates were recovered from the five *Apis florea* beehive samples. These isolates were subjected to an initial screening for antimicrobial activity using the soft-agar overlay technique. Of the strains tested, isolate BH111 exhibited the strongest antibacterial efficacy. Specifically, BH111 generated substantial zones of inhibition, 5.1 cm against *Staphylococcus aureus* TISTR885 (Fig. 1a) and an even larger 6.2 cm against *Bacillus cereus* TISTR687 (Fig. 1b), highlighting its powerful broad-spectrum potential.

Cultured on ISP-2 growth media, strain BH111 developed cream-coloured colonies and a white spore mass (Fig. 2a). The organism's cell wall consisted of the LL-isomer of 2,6-diaminopimelic acid. Analysis of whole-cell hydrolysates revealed the absence of diagnostic sugars, with only glucose and ribose being identified. Under light microscopy, the strain exhibited features characteristic of *Streptomyces* morphology. Its substrate mycelia were well-developed and branched and crucially, did not fragment into coccoid or bacillary elements. The strain also possessed rectiflexuous spore chains containing spores that ranged from spherical to oval in shape (Fig. 2b). The 16S rRNA (1485 nt) sequence analysis using BLAST showed that the BH111 strain is closely related to *S. kunmingensis* strain DSD1764 and strain DSD250 with 99.40% identity. The phylogenetic tree of the 16S rRNA sequence shared a cluster with *Streptomyces kunmingensis* (Fig. 3a). A phylogenetic tree based on *gyr*B gene sequences was also reconstructed (Fig. 3b). The *gyr*B sequence similarity

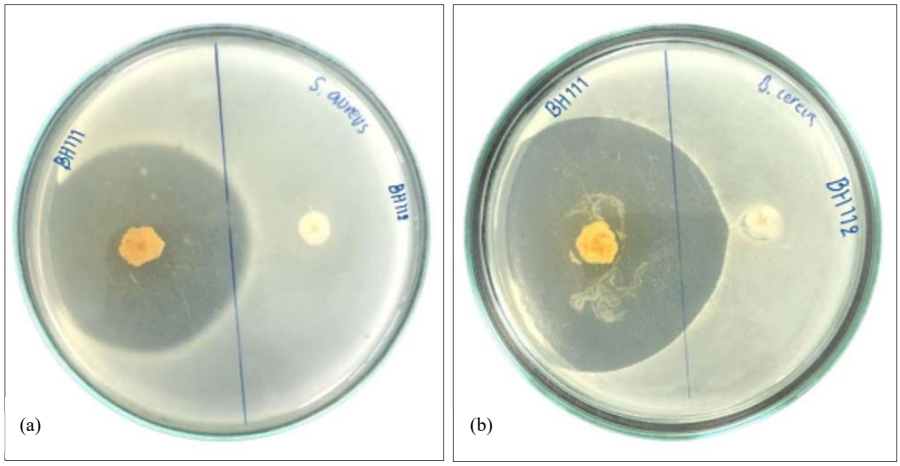

Fig. 1(a-b): Antibacterial activity of *Streptomyces kunmingensis* BH111 assessed by soft-agar overlay. The inhibitory effect of the actinomycete strain on two indicator bacteria, (a) Zone of inhibition formed against *Staphylococcus aureus* TISTR885 and (b) Inhibition against *Bacillus cereus* TISTR687

Assay utilized a 7 days old preculture of *S. kunmingensis* BH111 overlaid with soft agar containing the respective test bacterium on ISP-2 medium. Inhibition zone diameters were measured after 24 hrs of incubation at 37°C

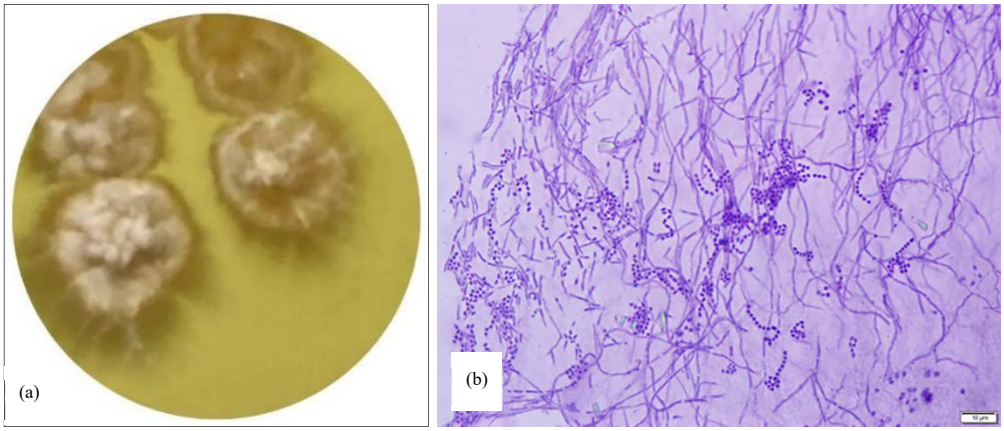

Fig. 2(a-b): Colony and microscopic observations of *Streptomyces kunmingensis* BH111. The key morphological attributes used for initial identification. These observations were made after 21 days of incubation on ISP-2 medium at 32°C, (a) Depicts the colony's appearance, notably its white spore mass and (b) Light micrograph showing the rectiflexuous spore chains and the shape of the individual spores (spherical to oval)
Scale bar in panel (b) represents 10 µm

between the BH111 strain and *Streptomyces kunmingensis* NRRL B-16240 (the type strain) was 99.52%. This high similarity, along with the similar 16S rRNA sequence, strongly suggests that BH111 is closely related to *Streptomyces kunmingensis*. Therefore, we designated BH111 as *Streptomyces kunmingensis* BH111. The 16S rRNA and *gyr*B gene sequences are accessible in GenBank under the accession numbers PP753780 and PQ231004, respectively. Comparison of physiological characteristics revealed similarities between *S. kunmingensis* BH111 and *S. kunmingensis* NRRL B-16240 (Table 1).

Analysis of the crude extract via Thin-Layer Chromatography-Direct Bioautography (TLC-DB) indicated the presence of at least two major antibacterial compounds active against the tested bacterial strains (Fig. 4a-c).

Purification of the *Streptomyces kunmingensis* BH111 crude extract yielded two distinct compounds. Their chemical structures were established using comprehensive spectroscopic analysis, as detailed below.

Compound 1: It was an orange powder; MP 314-315°C, ESI-MS (positive mode): m/z 375, $[M-H]^-$ (Calcd for $C_{22}H_{16}O_6$), m/z 375.0869 $[M-H]^-$; IRυ_{max} (KBr) cm^{-1}: 3440, 1633, 1600, 1572, 1379, 1287, 844, 571; UV (MeOH)λ_{max} nm: 268 and 289; ^{1}H-NMR (600 MHz, DMSO-d_6): δ_H: 14.55 (s, 1H, 7-OH), 14.36 (s, 1H, 3-OH), 14.07 (s, 1H, 5-OH), 11.40 (s br, 1H, 10-OH), 7.23 (s, 1H, 11-H), 7.01 (s, 1H, 8-H), 6.34 (s, 1H, 4-H), 2.90 (s, 3H, 9-CH_3), 1.56 (s, 6H, 1-CH_3); ^{13}C-NMR (125 MHz, DMSO-d_6): δ_C: 204.9 (C-2), 183.5(C-6), 170.7 (C-3), 170.5 (C-5), 167.6 (C-7), 162.1 (C-10), 152.7 (C-11a), 152.1 (C-9), 142.2 (C-2b), 139.1 (C6b), 128.5 (C-8), 128.4 (C-9a), 118.2 (C-11), 114.2 (C-11b), 107.1 (C-6a), 105.9 (C-5a), 102.1 (C-2a), 99.4 (C-4), 46.1 (C-1), 28.9 (2CH_3-1), 25.5 (CH_3-9).

Compound 2: It was a red powder; MP 179-180°C, ESI-MS (positive mode): m/z 335, $[M-H]^-$ (Calcd for $C_{19}H_{12}O_6$), m/z 335.0556 $[M-H]^-$; IRυ_{max} (KBr) cm^{-1}: 1703, 1625, 1558; UV (MeOH)λ_{max} nm: 242 and 274; ^{1}H-NMR (600 MHz, DMSO-d_6): δ_H: 14.62 (s br, 1H, 11-OH), 12.17 (s br, 1H, 1-OH), 7.68 (s, 1H, 6-H), 7.08 (d, J = 1.9, 1H, 9-H), 6.99 (d, J = 2.2, 1H, 4-H), 6.86 (d, J = 1.9, 1H, 7-H), 6.41 (d, J = 2.2, 1H, 2-H), 2.74 (s, 3H, 10-CH_3); ^{13}C-NMR (125 MHz, DMSO-d_6): δ_C: 187.4 (C-12), 180.8 (C-5), 166.3 (C-1), 165.9 (C-3), 164.2 (C-8), 159.5 (C-11), 141.0 (C-6a), 139.5 (C-10), 135.5 (C-4a), 127.7 (C-5a), 123.0 (C-6), 120.9 (C-9), 119.4 (C-10a), 111.3 (C-4), 108.7 (C-12a), 108.6 (C-2), 107.8 (C-7), 106.3 (C-11a), 24.2 (CH_3-10).

Structural analysis confirmed the identities of the two purified compounds: Compound **1** as resistomycin (or heliomycin) (Fig. 5a) and Compound **2** as tetracenomycin D (Fig. 5b). The production yield of these compounds by *Streptomyces kunmingensis* BH111 was quantified during isolation. Tetracenomycin D (Compound **2**) was the major product at a concentration of 1.56 mg/g of crude extract (1.14 mg/L of culture medium), followed by resistomycin (Compound **1**) at 1.16 mg/g of crude extract (1.10 mg/L of culture medium).

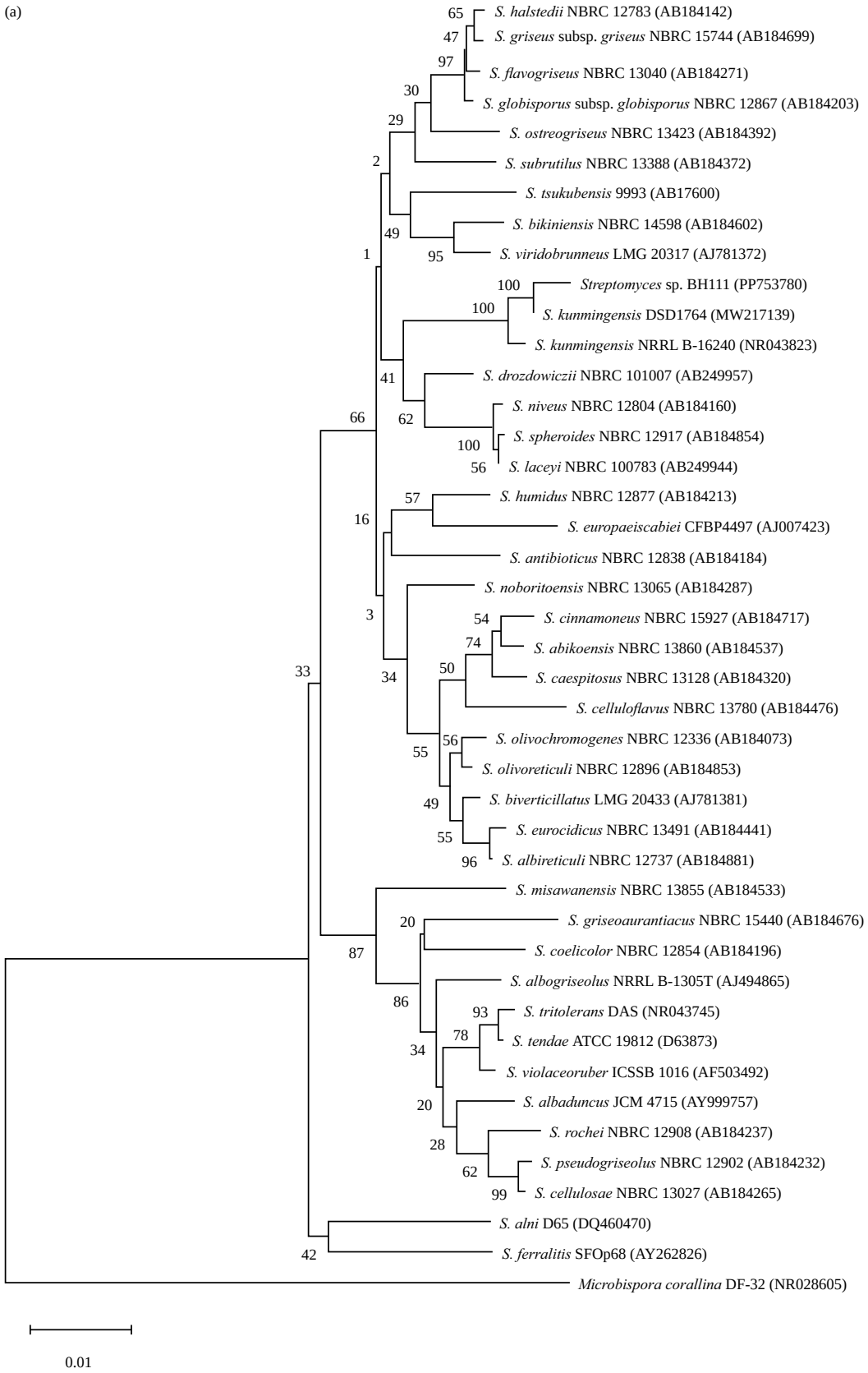

Fig. 3(a-b): Continue

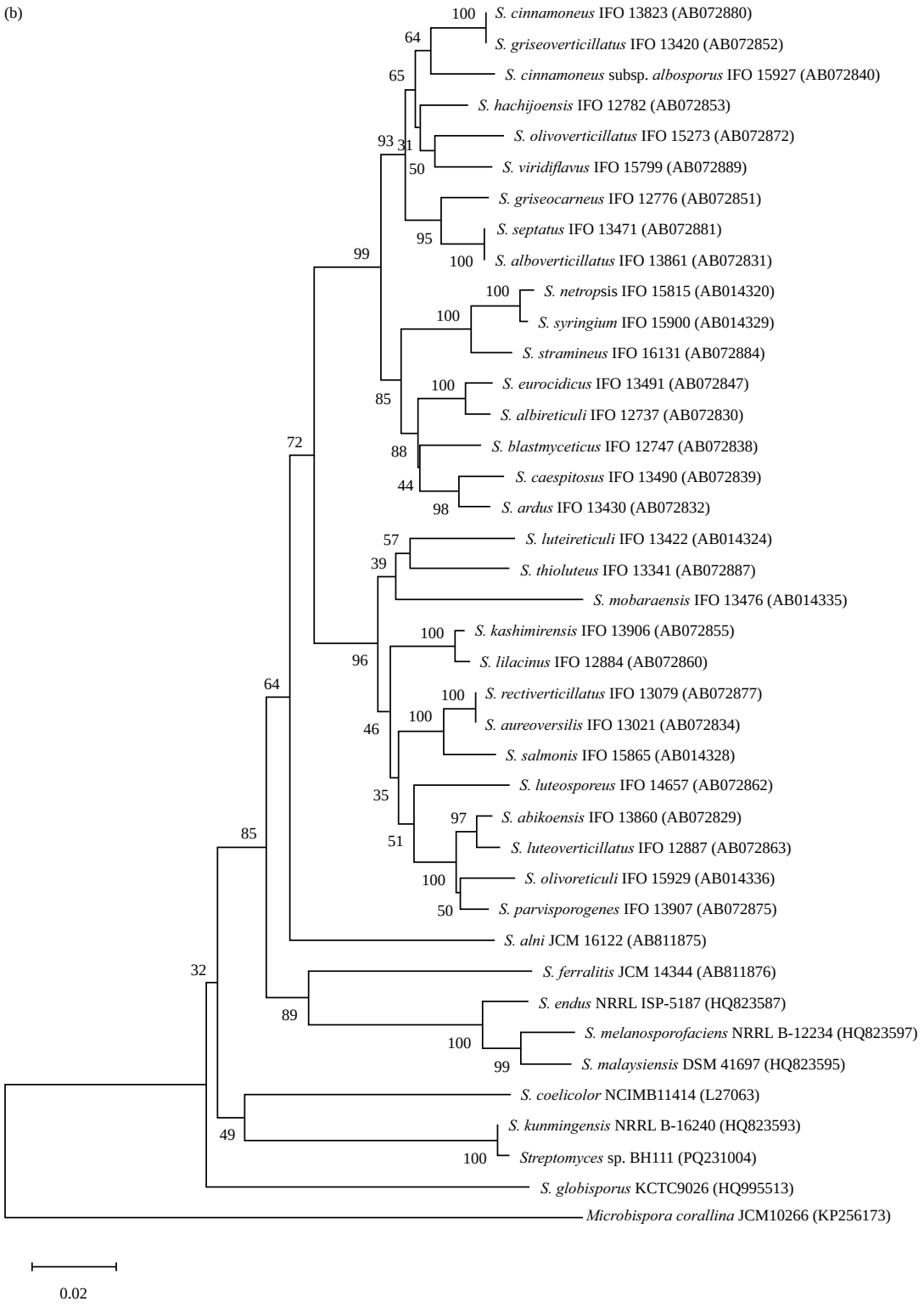

Fig. 3(a-b): Phylogenetic analysis of *Streptomyces kunmingensis* BH111. Trees were constructed using the Neighbor-Joining method in MEGA11 software to determine the evolutionary relationship of strain BH111 with closely related type strains (accession numbers are provided in parentheses), (a) Phylogenetic tree based on the 16S rRNA gene sequences and (b) Phylogenetic tree based on the *gyr*B gene sequences

Bootstrap values (1000 replicates) are indicated at the branch nodes. The scale bars represent (a) 0.01 and (b) 0.02 nucleotide substitutions per site

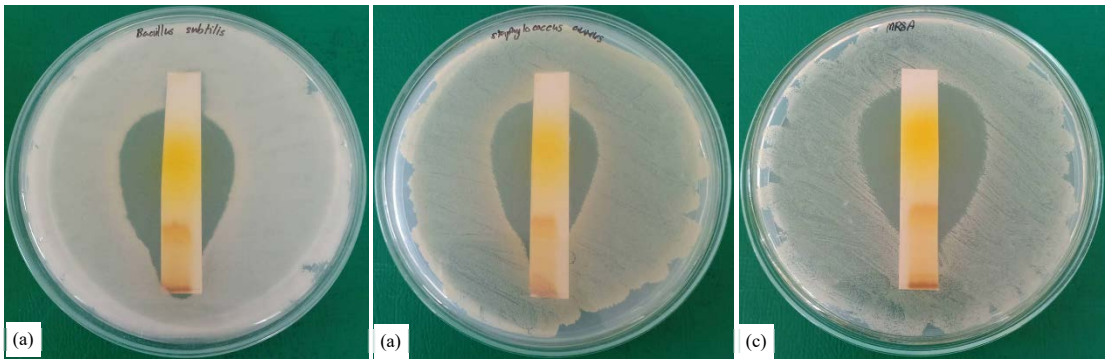

Fig. 4(a-c): Thin-layer chromatography (TLC) Bioautography of the crude extract. The antibacterial activity detected on the chromatogram after 24 hrs at 37°C of incubation at against three indicator strains, (a) *Bacillus subtilis* TISTR008, (b) *Staphylococcus aureus* TISTR885 and (c) Clinical isolate methicillin-resistant *S. aureus* (MRSA) Sp3

Table 1: Physiological characteristics of *S. kunmingensis* BH111 and *S. kunmingensis* NRRL B-16240*

Characteristics	BH111	NRRL B-16240
Degradation		
Adenine	+	+
Aesculin	+	+
Casein	+	+
Gelatin	-	-
Hypoxanthine	+	+
Starch	+	+
Tyrosine	+	+
Urea	-	-
Xanthine	+	+
Acid formation from		
Adonitol	-	-
L-arabinose	+	+
Cellobiose	+	+
Dulcitol	-	-
Meso-erythritol		
ND	-	
Fructose	+	+
Galactose	+	+
Glucose	+	+
Meso-inositol	W	+
D-lactose	+	+
Maltose	+	+
D-mannitol	+	+
Mannose	+	+
Melibiose	+	+
α-methyl-D-glucoside	ND	+
α-methyl-D-xyloside	ND	+
Raffinose	+	+
L-rhamnose	+	+
Salicin	ND	+
D-sorbitol	-	-
Sucrose	W	+
Trehalose	+	+
D-xylose	+	+
Growth at		
10°C	+	+
37°C	+	+
42°C	-	-

*Data from Goodfellow *et al.*[24], W: Weak positive after 24 hrs incubation and ND: Not determined

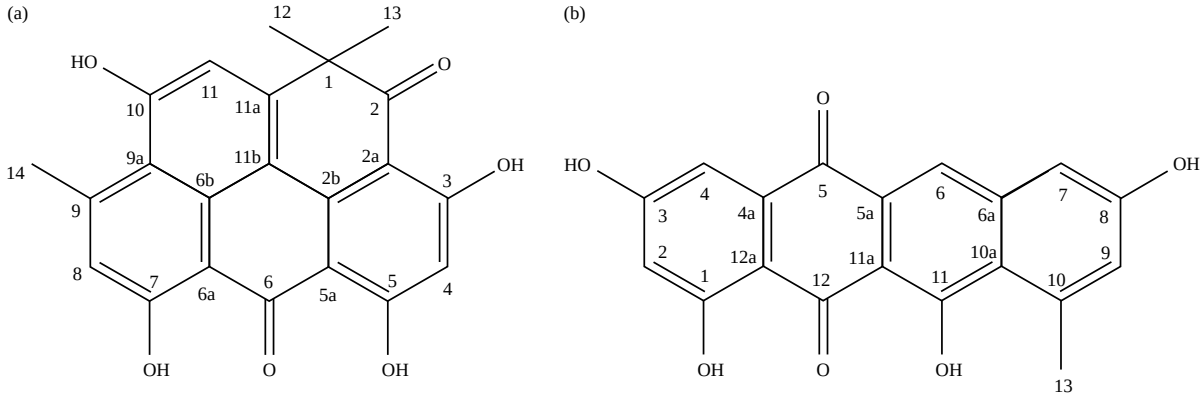

Fig. 5(a-b): Structures of the compounds, (a) Resistomycin and (b) Tetracenomycin D

Table 2: MIC and MBC of the purified compounds and chloramphenicol against tested bacteria

	MIC (µg/mL)			MBC (µg/mL)		
Test organisms	Compound **1**	Compound **2**	Chloramphenicol	Compound **1**	Compound **2**	Chloramphenicol
S. aureus TISTR885	16	32	2	128	256	16
S. epidermidis TISTR518	16	32	2	128	256	16
B. cereus TISTR687	16	32	2	128	256	16
B. subtilis TISTR008	16	32	2	128	256	16
E. coli TISTR887	64	256	16	256	>512	64
S. typhimurium TISTR292	64	256	16	256	>512	64
P. aeruginosa TISTR1287	128	512	32	512	>512	128
MRSA Sp3*	16	32	16	128	256	128

*Clinical isolate: Methicillin-resistant *S. aureus* strain Sp3

The antimicrobial efficacy of the crude extract and the two purified compounds was quantified using the microbroth dilution assay to determine minimum inhibitory concentrations (MICs) and minimum bactericidal concentrations (MBCs) against the panel of test bacteria. Both purified compounds exhibited a clear selective antibacterial activity against Gram-positive strains compared to Gram-negative strains. Compound **1** consistently displayed stronger antibacterial potency than Compound **2** across the board. The compounds demonstrated effective inhibitory activity against several Gram-positive strains. These targets included *Staphylococcus aureus* TISTR885, *S. epidermidis* TISTR518, *Bacillus cereus* TISTR687, *B. subtilis* TISTR008 and the Methicillin-resistant *S. aureus* (MRSA Sp3) clinical isolate. For these strains, the MICs ranged from 16 to 32 µg/mL and the MBCs ranged from 128 to 256 µg/mL. In contrast, the activity against Gram-negative bacteria was significantly lower, with MIC values falling between 64 and 512 and MBC values from 256 to >512 µg/mL (Table 2).

The cytotoxic potential of both the crude extract and its purified derivatives was assessed using a panel of four cell lines. This panel included one non-cancerous line (Vero) and three human carcinoma lines: MDA-MB-231 (breast), HeLa (cervical) and HepG2 (hepatocellular). Overall, the crude extract exhibited less cytotoxicity compared to the individual purified compounds.

Both purified compounds induced notable toxicity in both non-cancerous and cancerous lines. The values ranged from 12.03 to 29.62 µg/mL for the non-cancerous Vero cells and 10.72 to 27.57 µg/mL for the cancer lines. Consistent with the anticancer results, Compound **1** exhibited higher cytotoxic potency than Compound **2** against all cell lines tested. The selectivity indices (SI) for the crude extract and the purified compounds, ranging from 1.02 to 1.48 µg/mL, were consistently lower when tested against the MDA-MB-231 and HeLa cell lines. The SI is a crucial parameter, calculated as the ratio of toxicity to a non-cancerous cell line (Vero) to the toxicity against a cancerous cell line (IC_{50} non-cancer/IC_{50} cancer). A higher SI indicates a greater preference for targeting cancer cells over normal cells. In comparison, the reference drug, doxorubicin hydrochloride, yielded significantly higher SI values (14.68 and 29.25 µg/mL). These results collectively suggest that the tested extract and purified compounds have a comparatively reduced therapeutic window or a lower preference for selectively targeting these specific cancerous cell lines (Table 3).

Table 3: IC_{50} values and selectivity indices (SI) of crude extract and purified compounds against cancer cell lines

		MDA-MB-231 cells		HeLa cells		HepG2 cells	
	Vero cells						
Test substances	IC_{50} (µg/mL)	IC_{50} (µg/mL)	SI	IC_{50} (µg/mL)	SI	IC_{50} (µg/mL)	SI
Crude extract	21.47±7.74[a]	15.08±8.50[a]	1.42	14.54±8.23[a,b]	1.48	17.60±8.77[a]	1.22
Compound **1**	12.03±4.38[a]	11.81±7.33[a]	1.02	10.72±7.67[a,b]	1.12	12.42±6.32[a]	0.97
Compound **2**	29.62±12.18[a]	26.59±9.84[a]	1.11	25.36±10.15[a]	1.17	27.57±9.61[a]	1.07
Doxorubicin hydrochloride	117.60±32.28[b]	8.01±3.06[a]	14.68	4.02±1.93[b]	29.25	92.67±23.58[b]	1.27

Vero cells: African green monkey kidney cell line, MDA-MB-231 cells: Human breast cancer cell line, HeLa cells: Human cervical carcinoma cell line, HepG2: Human hepatocellular carcinoma cell line. IC_{50} values represent the concentration causing 50% growth inhibition. The values are expressed as Mean±Standard Deviation of the three replicates. SI: Selectivity indices (SI) were calculated as the ratio of the IC_{50} in the Vero cell line to the IC_{50} in the cancer cell lines. [a,b]Different letters indicated statistically significant differences within the same category ($p<0.05$)

Table 4: Results of predictions of molecular interaction between various topoisomerase II and the test compounds

			Hydrogen bonds			
Purified compounds	Binding energy (kcal/mol)	Interaction types	H-bond donors	H-bond acceptors	Bond length (A°)	Docking site
Compound **1**	-6.769	CoH	Asp479: HN	LIG: O	2.13083	Active pocket site
		CoH	LIG: H	Arg503: O	2.06045	
		CoH	LIG: H	Arg503: O	1.94175	
		Pi-An	Glu477: OE2 (negative)	LIG (Pi-orbitals)	4.96875	
		Pi-Al	LIG (Pi-orbitals)	Arg503 (Alkyl)	4.79788	
Compound **2**	-6.480	CoH	Ser480: HN	LIG: O	2.21439	Active pocket site
		CoH	LIG: H	Arg503: O	2.47156	
		CoH	LIG: H	Asp557: OD2	2.27287	
		Pi-Ca	Arg503: NH2 (positive)	LIG (Pi-orbitals)	4.93241	
		Pi-An	Asp479: OD1 (negative)	LIG (Pi-orbitals)	4.10144	
		Pi-An	Asp479: OD1 (negative)	LIG (Pi-orbitals)	4.25853	
		Pi-Al	LIG (Pi-orbitals)	Arg503 (Alkyl)	4.37837	
		Pi-Al	LIG (Pi-orbitals)	Arg503 (Alkyl)	4.42086	
Doxorubicin	-6.586	CoH	Asp479: HN	LIG: O	2.14562	Active pocket site
		CoH	Ser480: HN	LIG: O	1.99353	
		CoH	Gly776: HN	LIG: O	2.83489	
		CoH	Gly776: HN	LIG: O	1.99775	
		CoH	Gln778: HE21	LIG: O	2.59849	
		CoH	LIG: H	Gln778: OE1	2.80926	
		CoH	LIG: H	Asp479: OD1	1.99715	
		CaH	Gly478: HA2	LIG: O	3.01836	
		CaH	Gly776: HA2	LIG: O	2.50934	
		A	Ala779 (Alkyl)	LIG: C (Alkyl)	4.42443	
Amsacrine	-6.086	CoH	Asp479: HN	LIG: O	2.70433	Active pocket site
		CoH	Ser480: HN	LIG: O	2.05443	
		CoH	LIG: H	Glu477: OE2	2.17265	
		CaH	Gly478: HA1	LIG: O	3.02020	
		CaH	LIG: C	Asp557: OD1	3.40028	
		Pi-Al	LIG (Pi-orbitals)	Lys505 (Alkyl)	5.40247	

Topoisomerase II; PDB ID: 4G0U. Interaction types; CoH: Conventional hydrogen bond, CaH: Carbon hydrogen bond, A: Alkyl interaction, Pi-Al: Pi-Alkyl interaction, Pi-An: Pi-Anion interaction, Pi-Ca: Pi-Cation interaction. LIG; Ligand: Compounds **1**, **2**, doxorubicin and amsacrine

To investigate a potential anticancer mechanism, molecular docking simulations were performed to assess the interaction of Compounds **1** and **2** with the active site of human DNA topoisomerase II (PDB ID: 4G0U). Doxorubicin served as a positive control, while amsacrine (ASW) was used as the reference co-crystallized inhibitor. All four molecules demonstrated favorable binding energies within the topoisomerase II active site. The calculated relative binding energies were as follows: Compound **1** (-6.769 kcal/mol), doxorubicin (-6.586 kcal/mol), Compound **2** (-6.480 kcal/mol) and amsacrine (-6.086 kcal/mol). Complex stability was primarily driven by hydrogen bonds and hydrophobic interactions. Specific hydrogen bonding patterns included: Compound **1** formed hydrogen bonds with Asp479 and Arg503 (Fig. 6a-b). Compound **2** formed hydrogen bonds with Ser480, Arg503 and Asp557 (Fig. 6c-d). The positive control, doxorubicin, exhibited the highest number of hydrogen bond interactions overall, forming seven conventional and two carbon-hydrogen bonds with residues Gly478, Asp479, Ser480, Gly776 and Gln778 (Fig. 6e-f). Amsacrine formed three

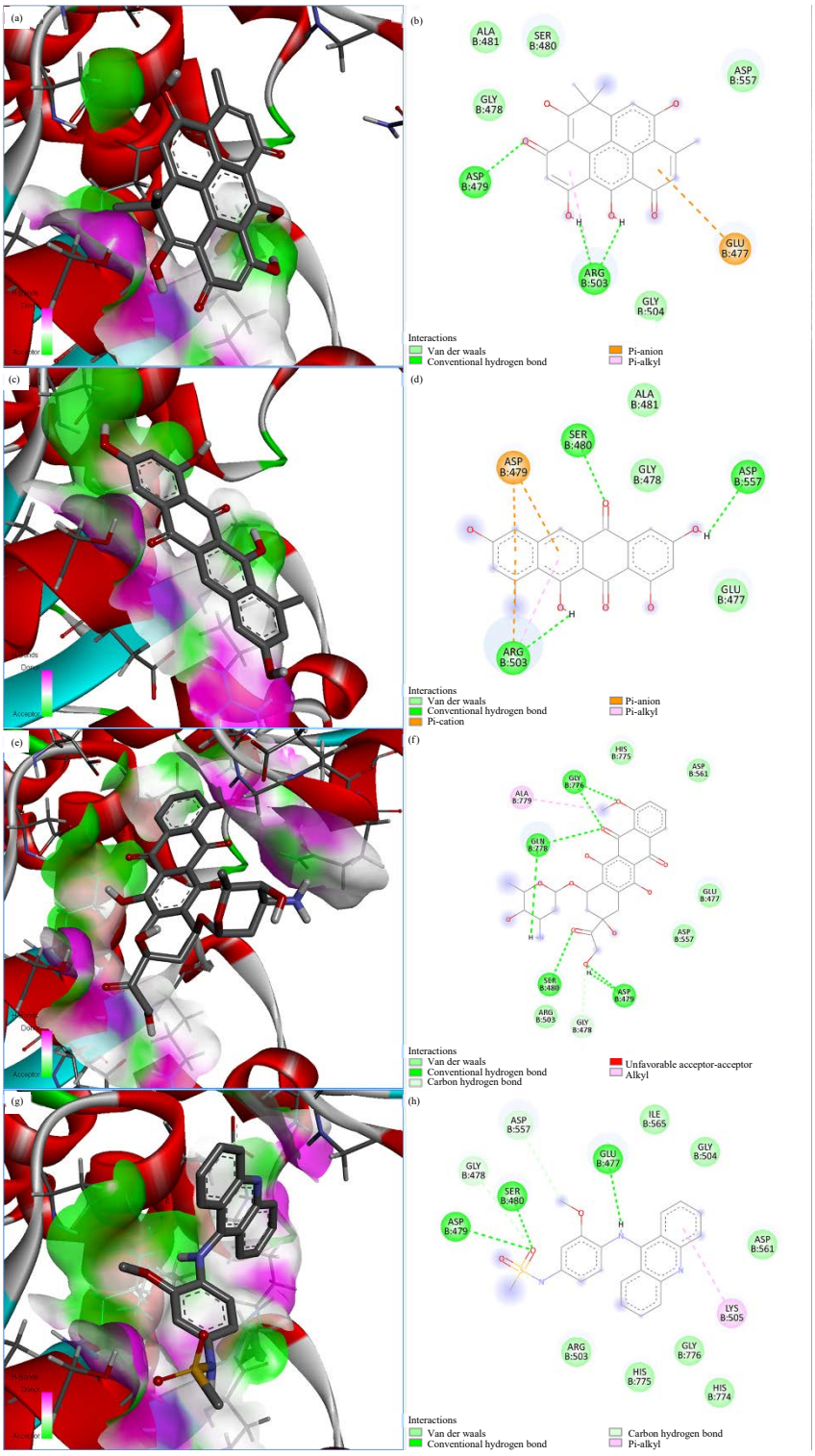

Fig. 6(a-h): Molecular docking analysis of ligands within the topoisomerase II active site. The binding interactions between the tested agents and the crystal structure of human DNA topoisomerase II, (a-b) Binding of Compound **1**, (c-d) Compound **2**, (e-f) Positive control, doxorubicin and (g-h) Reference inhibitor, amsacrine

For the three-dimensional (3D) illustrations: Hydrogen bond donors and acceptors are highlighted in pink and green, respectively. For the two-dimensional (2D) illustrations: Specific interactions are color-coded as follows: Conventional hydrogen bonds (dark green dashes), carbon hydrogen bonds (light green dashes), pi-stacked (deep pink), alkyl (pale pink), pi-alkyl (short pale pink), salt bridge (brown) and anion (long brown dashes). Amino acid residues involved in Van der Waals interactions are colored pale green

Table 5: Predicted absorption, distribution, metabolism, excretion and toxicity properties of the compound agents

	Compound agents			
Properties[a]	Compound **1**	Compound **2**	Amsacrine	Doxorubicin
TPSA	115.06	115.06	88.70	206.07
Consensus log $P_{o/w}$	2.89	2.36	3.47	0.50
Absorption				
Water solubility (log *S*)	-4.61	-4.98	-8.36	-5.20
Caco2 cell permeability (log Papp in 10^{-6} cm/sec)	0.397	-0.508	0.579	0.452
Human intestinal absorption (absorbed (%))	100	71.96	94.94	62.37
Skin permeability (log Kp cm/sec)	-2.735	-2.735	-2.734	-2.735
P-Glycoprotein substrate	Yes	Yes	Yes	Yes
P-Glycoprotein inhibitor	No	No	Yes	No
Distribution				
BBB permeability (log BBB)	-0.921	-1.004	-0.096	0.0328
Metabolism				
CYP2D6 substrate	No	No	No	No
CYP3A4 substrate	Yes	No	Yes	No
CYP1A2 inhibitor	No	Yes	Yes	No
CYP2C19 inhibitor	No	No	Yes	No
CYP2C9 inhibitor	No	No	Yes	No
CYP2D6 inhibitor	No	No	No	No
CYP3A4 inhibitor	No	No	Yes	No
Excretion				
Renal OCT2 substrate	No	No	No	No
Toxicity				
Ames_test	No	Mutagen	No	Mutagen
Carcino_mouse	No	No	No	No
Carcino_rat	No	Yes	No	No
TA100_10RLI	No	No	No	No
TA100_NA	No	No	No	No
TA1535_10RLI	No	No	No	No
TA1535_NA	No	No	No	No
hERG inhibitor	No	No	No	Medium risk
Hepatotoxicity	Yes	No	Yes	Yes
Skin sensitization	No	No	No	No

BBB: Blood-brain barrier, CYP: Cytochrome p450, Caco2: Caucasian colon adenocarcinoma cell line, hERG: Human ether-a-go-go-related gene, Kp: Skin permeability constant, log $P_{o/w}$: Log of relative solubility of the drug in n-octanol, OCT2: Organic cation transporter 2 and TPSA: Topological polar surface area

conventional and two carbon-hydrogen bonds with Glu477, Gly478, Asp479 and Ser480 and Asp557 (Fig. 6g-h). The molecular docking analysis against topoisomerase II provided significant insight into the compounds' potential activity. Both compounds exhibited favorable binding energies, a metric where more negative values indicate a stronger predicted affinity. Compound **1** showed the highest predicted affinity (-6.769 kcal/mol), slightly surpassing the positive control, doxorubicin (-6.586 kcal/mol) and also the activity of Compound **2** (-6.480 kcal/mol). Crucially, the predicted binding of both isolated compounds exceeded that of the small-molecule inhibitor, amsacrine (-6.086 kcal/mol), suggesting a more stable interaction with the target. Docking results showed that the molecular structure of both compounds is well-suited for binding to the target protein. This favorable interaction is thought to be responsible for the compounds' anticancer activity, while Table 4 summarizes the precise binding characteristics, including hydrogen bond specifics and the participating amino acid residues.

The ADMET analysis (Absorption, Distribution, Metabolism, Excretion and Toxicity) was conducted for Compounds **1**, **2**, amsacrine and doxorubicin using predictive tools (SwissADME, Pre-ADMET and pkCSM). The predicted ADMET parameters for both isolated compounds were evaluated to assess their potential as oral drug candidates; these critical values are fully detailed in Table 5. Both compounds showed promising absorption profiles. Compound **1** achieved a perfect predicted human intestinal absorption (HIA) of 100.00%, while Compound **2** was also high at 71.96%. Furthermore, both compounds were predicted to exhibit moderate Caco-2 cell permeability (log Papp $<8\times10^{6}$ cm/sec) and high skin permeability (log Kp <-2.5). Regarding drug distribution, both compounds were predicted to have limited blood-brain barrier (BBB) penetration (logBBB <0.3). A potential limitation to oral bioavailability was identified in the prediction that both compounds function as P-glycoprotein (P-gp) substrates, although neither was predicted to be a P-gp inhibitor. The metabolic profiles

indicated distinct differences: Compound **1** was predicted to be a substrate of CYP3A4, while Compound **2** was predicted to inhibit CYP1A2. Toxicity predictions flagged several concerns: Compound **2** was predicted to be mutagenic in the Ames test and potentially carcinogenic in rats and Compound **1** was flagged for potential hepatotoxicity. However, a positive finding was the prediction that both compounds would not inhibit the hERG channel, suggesting a potentially low risk of cardiotoxicity. This finding, along with all others, requires subsequent *in vitro* confirmation.

DISCUSSION

This investigation successfully isolated and identified two known anthraquinone derivatives, resistomycin (or heliomycin) (Compound **1**) and tetracenomycin D (Compound **2**), from the *Apis florea*-derived isolate, *Streptomyces kunmingensis* BH111. The identity of these compounds was unequivocally confirmed by comparing their comprehensive spectral data with those reported in existing literature, such as the resistomycin and tetracenomycin D isolated from the marine actinobacterium *Streptomyces corchorusii* AUBN$_1$/7[21]. This finding is noteworthy as resistomycin and tetracenomycin D have been reported from various *Streptomyces* strains across diverse habitats, including marine sediment, termite guts, saline soil and humus soils[22-24]. This study contributes a new producing organism, *S. kunmingensis* BH111, isolated from a honeybee hive environment.

Phylogenetic analysis, incorporating both 16S rRNA and *gyr*B gene sequences, firmly established the close relationship of strain BH111 to known *S. kunmingensis* strains (e.g., DSD1764 and NRRL B-16240[25]). While *S. kunmingensis* has been previously studied for metabolites like endophenazine A and actinomycin-type compounds with cytotoxic and antimicrobial activities[26,27], our study represents the first report of this species producing resistomycin and tetracenomycin D.

The yield of these compounds can be highly variable depending on the *Streptomyces* species and culture conditions. Our isolation of *S. kunmingensis* BH111 from an *Apis florea* beehive yielded resistomycin at 1.16 mg/g of crude extract and tetracenomycin D at 1.56 mg/g of crude extract. While these yields are lower than some reported maximums (e.g., for resistomycin from *S. canus* BYB02[22]), they are comparable to or higher than others found in the literature, such as those from *Streptomyces* sp., SP9[28], underscoring the potential of this strain.

The isolated anthraquinone derivatives displayed selective antibacterial activity, being more potent against Gram-positive bacteria than Gram-negative bacteria. This result is consistent with previous reports on resistomycin and tetracenomycin D[21,23,24]. The differential susceptibility is primarily attributed to the structural differences in bacterial cell envelopes: The lipopolysaccharide outer membrane of Gram-negative bacteria restricts the uptake of lipophilic molecules, making Gram-positive bacteria, with their more permeable peptidoglycan layer, more vulnerable[29]. The known antimicrobial mechanisms of these compounds include disruption of bacterial fatty acid synthase (FAS), interference with peptidoglycan synthesis and destabilization of cell membranes and biofilm-forming proteins[30,31].

Beyond their antimicrobial action, resistomycin and tetracenomycin D are known for their anticancer potential[24,32]. Our results confirmed the cytotoxic activity of both compounds against MDA-MB-231, HeLa and HepG2 cancer cell lines, with values ranging from 10.72 to 27.57 µg/mL. These findings align with prior research showing potent cytotoxicity of resistomycin against various cell lines[32]. However, a significant cautionary finding was the similar cytotoxicity observed against non-cancerous Vero cells (IC_{50} range: 12.03 to 29.62 µg/mL). This low distinction translated to a low selectivity index (SI) (0.97 to 1.17) compared to doxorubicin hydrochloride, suggesting a poor therapeutic window and a need for further structural modification to enhance cancer-specific targeting.

To probe the mechanism underpinning the observed cytotoxicity, molecular docking simulations were conducted against human DNA topoisomerase II (PDB ID: 4G0U), a common therapeutic target for anthraquinone-based drugs[27,33]. Both Compound **1** (-6.769 kcal/mol) and Compound **2** (-6.480 kcal/mol) showed favorable binding affinities. Notably, Compound **1** exhibited stronger binding than both doxorubicin (-6.586 kcal/mol) and the reference inhibitor amsacrine (-6.086 kcal/mol), while Compound **2** was slightly weaker than doxorubicin.

The binding stability was primarily mediated by hydrogen bonds involving key residues within the active pocket. Specifically, hydroxyl groups (such as the C5 position of Compound **1** and the C11 position of Compound **2**) formed crucial hydrogen bonds with residues like and others (Arg503, Glu477, Asp479, Ser480 and Asp557). These interactions support the hypothesis that both anthraquinone derivatives may function as topoisomerase II inhibitors, contributing to their anticancer effect. This mechanism is supported by other studies, which have also reported alternative pathways, including the inhibition of Histone Deacetylases (HDACs)[34] and the induction of apoptosis and phase arrest via the and MAPK signaling pathways[35].

The prediction of ADMET properties provides essential early-stage insight into the drug-likeness of the compounds. The analysis suggested promising oral absorption characteristics, with both Compound **1** (100.00%) and Compound **2** (71.96%) showing high predicted human intestinal absorption, which surpasses the prediction for doxorubicin (62.37%). The compounds were predicted to be P-glycoprotein substrates but not inhibitors, suggesting that while efflux may reduce bioavailability, the risk of drug-drug interactions is lower[36]. Both compounds were predicted to have limited blood-brain barrier (BBB) penetration (logBBB <0.3), limiting potential CNS activity[37]. In terms of Metabolism, Compound **1** was predicted to be a substrate of CYP3A4 and Compound **2** was predicted to inhibit CYP1A2. These results flag potential drug metabolism issues. For Toxicity, Compound **2** was predicted to be mutagenic in the Ames test and potentially carcinogenic in rats. Furthermore, Compound **1** was flagged for potential hepatotoxicity. Encouragingly, both compounds were predicted not to inhibit the channel, suggesting a lower risk of cardiotoxicity, though this requires *in vitro* confirmation[38].

The ADMET profile indicates favorable initial absorption but necessitates further research to mitigate potential concerns regarding interaction and hepatotoxicity risk during optimization. The *Apis florea* beehive niche has proven to be a valuable source for isolating *S. kunmingensis* BH111, a producer of these structurally intriguing and biologically active anthraquinone derivatives.

CONCLUSION

This study successfully isolated *Streptomyces kunmingensis* BH111 from an *Apis florea* beehive, establishing a new source and habitat association for this bacterial species. The strain was confirmed through comprehensive taxonomic and phylogenetic analysis, including 16S rDNA and *gyr*B gene sequencing. Further investigation led to the purification and structural elucidation of two potent bioactive metabolites: The anthraquinone derivatives resistomycin (or heliomycin) (Compound **1**) and tetracenomycin D (Compound **2**). This is the first report of *S. kunmingensis* producing these specific compounds. The purified compounds exhibited significant and selective antibacterial activity against Gram-positive bacteria, including the clinical isolate MRSA Sp3. Furthermore, they demonstrated substantial cytotoxic activity against the tested human cancer cell lines (MDA-MB-231, HeLa and HepG2). Molecular docking simulations provided a plausible mechanism for this anticancer activity, suggesting that both compounds act as potent inhibitors of human DNA topoisomerase II. However, the low selectivity index (SI) observed across the cytotoxicity assays, coupled with potential ADMET concerns (specifically CYP450 interactions and predicted hepatotoxicity for Compound **1**), indicates that these compounds require chemical modification and targeted delivery strategies before they can be considered safe and selective therapeutic candidates. Overall, the *Apis florea* beehive niche has proven to be a valuable resource for discovering novel producers of biologically active anthraquinone compounds.

SIGNIFICANCE STATEMENT

The discovery of the novel strain *Streptomyces kunmingensis* BH111 from an *Apis florea* beehive underscores this unique environment as a vital and often overlooked niche for bioprospecting. This strain is the first of its species confirmed to produce the highly active anthraquinone derivatives resistomycin and tetracenomycin D. These compounds demonstrated potent efficacy against drug-resistant bacteria (including MRSA) and human cancer cells by acting as putative topoisomerase II inhibitors, thereby providing promising natural product scaffolds for developing urgently needed antimicrobial and anticancer drugs.

ACKNOWLEDGMENT

This work was supported by a research grant (No. SRIF-JRG-2568-08) from the Faculty of Science, Silpakorn University, Nakhon Pathom, Thailand.

REFERENCES

1. Selim, M.S.M., S.A. Abdelhamid and S.S. Mohamed, 2021. Secondary metabolites and biodiversity of actinomycetes. J. Genet. Eng. Biotechnol., Vol. 19. 10.1186/s43141-021-00156-9.
2. Grubbs, K.J., D.S. May, J.A. Sardina, R.K. Dermenjian and T.P. Wyche *et al*., 2021. Pollen *Streptomyces* produce antibiotic that inhibits the honey bee pathogen *Paenibacillus larvae*. Front. Microbiol., Vol. 12. 10.3389/fmicb.2021.632637.
3. Santos-Beneit, F., A. Ceniceros, A. Nikolaou, J.A. Salas and J. Gutierrez-Merino, 2022. Identification of antimicrobial compounds in two *Streptomyces* sp. strains isolated from beehives. Front. Microbiol., Vol. 13. 10.3389/fmicb.2022.742168.

4. Promnuan, Y., S. Promsai, W. Pathom-Aree and S. Meelai, 2021. *Apis andreniformis* associated actinomycetes show antimicrobial activity against black rot pathogen (*Xanthomonas campestris* pv. *campestris*). PeerJ, Vol. 9. 10.7717/peerj.12097.
5. Hockett, K.L. and D.A. Baltrus, 2017. Use of the soft-agar overlay technique to screen for bacterially produced inhibitory compounds. J. Visualized Exp., Vol. 119. 10.3791/55064.
6. Taechowisan, T., W. Puckdee and W.S. Phutdhawong, 2019. *Streptomyces zerumbet*, a novel species from *Zingiber zerumbet*(L.) Smith and isolation of its bioactive compounds. Adv. Microbiol., 9: 194-219.
7. Jesionek, W., Á.M. Móricz, Á. Alberti, P .G. Ott, B. Kocsis, G. Horváth and I.M. Choma, 2015. TLC-direct bioautography as a bioassay guided method for investigation of antibacterial compounds in *Hypericum perforatum* L. J. AOAC Int., 98: 1013-1020.
8. Becker, B., M.P. Lechevalier, R.E. Gordon and H.A. Lechevalier, 1964. Rapid differentiation between *Nocardia* and *Streptomyces* by paper chromatography of whole-cell hydrolysates. Appl. Microbiol., 12: 421-423.
9. Boone, C.J. and L. Pine, 1968. Rapid method for characterization of actinomycetes by cell wall composition. Appl. Microbiol., 16: 279-284.
10. Taechowisan, T., T. Chuen-Im and W.S. Phutdhawong, 2024. Antioxidant and antibacterial properties of 1,3-dihydroxy-,2',2'-dimethylpyrano-(5,6)-xanthone from *Streptomyces* sp. SU84. Pak. J. Biol. Sci., 27: 132-141.
11. Yamamoto, S. and S. Harayama, 2020. PCR amplification and direct sequencing of *gyrB* genes with universal primers and their application to the detection and taxonomic analysis of *Pseudomonas putida* strains. Appl. Environ. Microbiol., 61: 3768-3768.
12. Tamura, K., G. Stecher and S. Kumar, 2021. MEGA11: Molecular evolutionary genetics analysis version 11. Mol. Biol. Evol., 38: 3022-3027.
13. Pfaller, M.A., R.N. Jones, D.H. Walter and Q.C.S. Group, 2001. Proposed quality control guidelines for National Committee for Clinical Laboratory Standards Susceptibility Tests using the veterinary antimicrobial agent tiamulin. Diagn. Microbiol. Infect. Dis., 40: 67-70.
14. van Meerloo, J., G.J.L. Kaspers and J. Cloos, 2011. Cell Sensitivity Assays: The MTT Assay. In: Cancer Cell Culture: Methods and Protocols, Cree, I.A. (Ed.), Humana Press, Totowa, New Jersey, United States, ISBN: 978-1-61779-079-9, pp: 237-245.
15. Li, Z.Y., G.S. Xu and X. Li, 2021. A unique topoisomerase II inhibitor with dose-affected anticancer mechanisms and less cardiotoxicity. Cells, Vol. 10. 10.3390/cells10113138.
16. Pettersen, E.F., T.D. Goddard, C.C. Huang, G.S. Couch, D.M. Greenblatt, E.C. Meng and T.E. Ferrin, 2004. UCSF chimera-A visualization system for exploratory research and analysis. J. Comput. Chem., 25: 1605-1612.
17. Daina, A., O. Michielin and V. Zoete, 2017. SwissADME: A free web tool to evaluate pharmacokinetics, drug-likeness and medicinal chemistry friendliness of small molecules. Sci. Rep., Vol. 7. 10.1038/srep42717.
18. Lamie, P.F. and J.N. Philoppes, 2021. Design, synthesis, stereochemical determination, molecular docking study, *in silico* pre-ADMET prediction and anti-proliferative activities of indole-pyrimidine derivatives as Mcl-1 inhibitors. Bioorg. Chem., Vol. 116. 10.1016/j.bioorg.2021.105335.
19. Pires, D.E.V., T.L. Blundell and D.B. Ascher, 2015. pkCSM: Predicting small-molecule pharmacokinetic and toxicity properties using graph-based signatures. J. Med. Chem., 58: 4066-4072.
20. Adinarayana, G., M.R. Venkateshan, V.V.S.N.K. Bapiraju, P. Sujatha, J. Premkumar, P. Ellaiah and A. Zeeck, 2006. Cytotoxic compounds from the marine actinobacterium *Streptomyces corchorusii* AUBN$_1$/7^1. Russ. J. Bioorg. Chem., 32: 295-300.
21. Zhang, Y.I., S. Li, D.H. Jiang, L.C. Kong, P.H. Zhang and J.D. Xu, 2013. Antifungal activities of metabolites produced by a termite-associated *Streptomyces canus* BYB02. J. Agric. Food Chem., 61: 1521-1524.
22. Sajid, I., K.A. Shaaban and S. Hasnain, 2011. Antitumour compounds from a saline soil isolate, *Streptomyces griseoincarnatus* CTF15. Nat. Prod. Res., 25: 549-559.
23. Vijayabharathi, R., P. Bruheim, T. Andreassen, D.S. Raja, P.B. Devi, S. Sathyabama and V.B. Priyadarisini, 2011. Assessment of resistomycin, as an anticancer compound isolated and characterized from *Streptomyces aurantiacus* AAA5. J. Microbial., 49: 920-926.
24. Goodfellow, M., S.T. Williams and G. Alderson, 1986. Transfer of *Chainia* species to the genus *Streptomyces* with emended description of species. Syst. Appl. Microbiol., 8: 55-60.
25. Wei, H.X., X.W. Fang, X.S. Xie, S.P. Zhang, Y. Jiang and S.H. Wu, 2017. Secondary metabolites of a soil-derived *Streptomyces kunmingensis*. Chem. Nat. Compd., 53: 794-796.
26. Sangeetha, M., S. Sasirekha, J. Mahendran, A. Sivarajan and M. Radhakrishnan *et al*., 2025. Multifunctional metabolites of *Streptomyces kunmingensis* BS19 from bamboo rhizosphere soil. Int. Microbiol., Vol. 28. 10.1007/s10123-024-00619-2.
27. Abdelfattah, M.S., M.I.Y. Elmallah, A.H.I. Faraag, A.M.S. Hebishy and N.H. Ali, 2018. Heliomycin and tetracinomycin D: Anthraquinone derivatives with histone deacetylase inhibitory activity from marine sponge-associated *Streptomyces* sp. SP9 3 Biotech, Vol. 8. 10.1007/s13205-018-1304-1.

28. Yilmaz, E.I., M. Yavuz and M. Kizil, 2008. Molecular characterization of rhizospheric soil streptomycetes isolated from indigenous Turkish plants and their antimicrobial activity. World J. Microbiol. Biotechnol., 24: 1461-1470.
29. Qun, T., T. Zhou, J. Hao, C. Wang and K. Zhang *et al*., 2023. Antibacterial activities of anthraquinones: Structure-activity relationships and action mechanisms. RSC Med. Chem., 14: 1446-1471.
30. Badran, A.R., S.A. Ali, H.Y. Ebrahim, A.M.S. Hebishy, E.A. Essawy and M.S. Abdelfattah, 2023. Isolation and structure elucidation of aromatic polyketides from marine actinomycete with antibiofilm activity against *Staphylococcus aureus* and *Escherichia coli*. Egypt. J. Chem., 66: 303-311.
31. Abu Zaid, A.S., M.A. Yassien, K.M. Aboshanab and A.M. Elissawy, 2021. *Streptomyces variabilis* isolate MW091521: A new microbial source of heliomycin. Appl. Biochem. Microbiol., 57: 564-570.
32. Fisher, G.R., J.R. Brown and L.H. Patterson, 1990. Involvement of hydroxyl radical formation and DNA strand breakage in the cytotoxicity of anthraquinone antitumour agents. Free Radical Res. Commun., 11: 117-125.
33. Mueller, S.O. and H. Stopper, 1999. Characterization of the genotoxicity of anthraquinones in mammalian cells. Biochim. Biophys. Acta-Gen. Subj., 1428: 406-414.
34. Han, Z., X. Zhao, E. Zhang, J. Ma and H. Zhang *et al*., 2021. Resistomycin induced apoptosis and cycle arrest in human hepatocellular carcinoma cells by activating p38 MAPK pathway *in vitro* and *in vivo*. Pharmaceuticals, Vol. 14. 10.3390/ph14100958.
35. Aloufi, A.S., O.A. Habotta, M.S. Abdelfattah, M.N. Habib and M.M. Omran *et al*., 2023. Resistomycin suppresses prostate cancer cell growth by instigating oxidative stress, mitochondrial apoptosis, and cell cycle arrest. Molecules, Vol. 28. 10.3390/molecules28237871.
36. Dewanjee, S., T.K. Dua, N. Bhattacharjee, A. Das and M. Gangopadhyay *et al*., 2017. Natural products as alternative choices for P-glycoprotein (P-gp) inhibition. Molecules, Vol. 22. 10.3390/molecules22060871.
37. Elmaidomy, A.H., H.A. Alhadrami, E. Amin, H.F. Aly and A.M. Othman *et al*., 2020. Anti-inflammatory and antioxidant activities of terpene- and polyphenol-rich *Premna odorata* leaves on alcohol-inflamed female wistar albino rat liver. Molecules, Vol. 25. 10.3390/molecules25143116.
38. de Sousa Santana, L.E.G., I.K.I. Miranda and J.A. Sousa, 2020. *In silico* analysis of the pharmacokinetics, pharmacodynamics and toxicity of two compounds isolated from *Moringa oleífera*. Res. Soc. Dev., Vol. 9. 10.33448/rsd-v9i11.10469.